EUROFUSION WP14ER-PR(15) 13905

C Rea et al.

Comparative studies of electrostatic turbulence induced transport in presence of Resonant Magnetic Perturbations in RFX-mod

Preprint of Paper to be submitted for publication in
Nuclear Fusion

This work has been carried out within the framework of the EUROfusion Consortium and has received funding from the Euratom research and training programme 2014-2018 under grant agreement No 633053. The views and opinions expressed herein do not necessarily reflect those of the European Commission.

Comparative studies of electrostatic turbulence induced transport in presence of Resonant Magnetic Perturbations in RFX-mod

C. Rea[1], N. Vianello[1,2], M. Agostini[1], R. Cavazzana[1], G. De Masi[1], E. Martines[1], B. Momo[1], P. Scarin[1], S. Spagnolo[1], G. Spizzo[1], M. Spolaore[1], M. Zuin[1]

[1]*Consorzio RFX (CNR, ENEA, INFN, Università di Padova, Acciaierie Venete SpA)*
Corso Stati Uniti 4 - 35127 Padova, Italy

[2]*Ecole Polytechnique Fédérale de Lausanne (EPFL),*
Centre de Recherches en Physique des Plasmas (CRPP), CH-1015 Lausanne, Switzerland

Abstract

Three-dimensional non-axisymmetric magnetic fields are purposely applied to toroidally symmetric fusion plasmas in order to modify transport of heat and particle fluxes to the plasma-facing components (PFCs), and specifically to control and suppress Edge Localized Modes (ELMs) in H-mode tokamak plasmas. This paper presents a comparative study between two magnetic configurations available in the RFX-mod device, namely the original reversed-field pinch configuration and the more recent low-field circular ohmic tokamak. The object of this study is the chaotic edge, which is spontaneous in the RFP configuration and induced by externally applied magnetic perturbations (MPs) in the tokamak. The analogy between the RFX-mod reversed-field pinch and tokamak configuration is developed through experiments with externally applied Resonant Magnetic Perturbations (RMPs). A detailed study of the underlying magnetic topology in both configurations is given through the field line tracing code FLiT. The electrostatic flux profiles turn out to be modulated around the O-point and X-point of the magnetic islands driven by the externally applied perturbations. Furthermore, the evidence of transport induced by small-scale electrostatic turbulence is discussed and the transverse wave numbers characterizing it are identified.

1. Introduction

In present fusion devices, independently of the magnetic configuration, magnetic perturbations (MPs) are applied in order to modify transport of heat and particle fluxes to the plasma-facing components (PFCs). This is particularly true for the tokamak discharges, where the H-Mode is accompanied by plasma instabilities, known as Edge Localized Modes (ELMs) which cause repetitive release of particle and heat in the scrape-off layer towards the wall and the divertor plates [1–3]. The MP approach has proved to be a successful ELM suppression technique in several existing devices such as JET [4, 5], ASDEX Upgrade [6], DIII-D [7, 8], MAST [9],

KSTAR [10] and NSTX [11]. Such technique, moreover, is foreseen to be crucial for ITER, as well.

According to the standard peeling-ballooning theory, ELM appearance is ultimately due to too steep pedestal gradients that develop in the H-mode regime [12]. In order to limit these gradients, magnetic perturbations with a non negligible radial component are produced, which enhance the radial transport through the much more efficient parallel transport. When MPs are applied, magnetic field lines start to exhibit a chaotic behavior: at the edge conserved flux surfaces are destroyed, giving rise to a *stochastic* or *ergodic* layer that helps to control and avoid ELMs by flattening the pressure profile.

The edge ergodization obtained for example in TEXTOR [13], and more generally the island divertor concept applicable in RFP devices [14] as well as in stellarators [15], share the same rationale: a non-axisymmetric magnetic field at the edge distributes the plasma-wall interaction (PWI), which is also exploited to manage impurity removal and to withstand higher power fluxes obtained during improved confinement regimes.

In the presence of externally applied MPs, the link between magnetic topology and transport properties is of fundamental importance in all devices. Indeed, some drawbacks of MP application are well-known: density pump-out often limits plasma confinement [8]; plasma response to MPs depends on collisionality, so the extrapolation to ITER is still uncertain [16]; finally, a strong electrostatic response to magnetic islands is known since early experiments of MP application [17, 18]; furthermore, in more recent experiments on TEXTOR and RFX-mod [19–21] it has been confirmed that in the presence of applied MPs convective transport can be produced orders of magnitude larger than usual chaotic radial diffusion. A detailed analysis of the effects of MP application is therefore mandatory to correctly extrapolate to ITER.

In this contribution, we will present further evidence on how MP fields can strongly affect and influence particle and energy transport in the plasma edge of RFX-mod, operated both as a reversed-field pinch and as an ohmic circular tokamak. We will focus on the role of electrostatic fluctuations in edge transport mechanisms by describing how this specific transport channel can be affected by the application of external 3D fields. We will see that the electrostatic fluxes turn out to be modulated around the O-point and the X-point of the outermost island, therefore the flux modulation in the presence of resonant MP fields is a common physical feature despite the different magnetic geometry, accordingly to what has been discussed in [20, 22]. Furthermore, we will provide information about the typical transverse wave numbers of the fluctuations of electrostatic particle and energy fluxes in both the RFP and the tokamak configuration. More in detail, we will give a specific description of transport around the O-point and X-point regions

of the island of the applied resonant perturbations developing a comparative study between the two configurations of the RFX-mod device.

The paper is organized as follows. Section 2 describes the experimental setup, the RFX-mod device and the diagnostics that have been used. Section 3 introduces the reference frame used to give a meaningful interpretation of measurements with respect to the underlying topology. In Section 4 properties of transport driven by electrostatic fluctuations in both magnetic configurations are described and proof of the modulation of the electrostatic fluxes is discussed by focusing on the reconstructed underlying magnetic topology. In Section 5 we describe more in detail the flux modulation by discussing the transport contributions coming from small scale electrostatic turbulence. Finally, in Section 6 conclusions are drawn.

2. Experimental setup and diagnostics

The RFX-mod device [23] ($a = 0.46$ m and $R = 2$ m, minor and major radii respectively) is the largest Reversed Field Pinch device in operation. It is equipped with a highly flexible feedback control system for MHD control, based on 192 active saddle coils that cover the whole plasma boundary [24]. It has been shown that, at high plasma current ($I_p \geq 1$ MA in RFX-mod), the RFP exhibits a transition from a dynamic regime of Multiple Helicity states (MH mode, characterized by a broad spectrum of tearing modes) towards a helical equilibrium, the so-called Single Helicity (SH) state [25–27], set by a single tearing mode together with its higher order harmonics. The amplitude of this mode is sufficient to modify the flux surfaces, creating a helical core with reduced chaos surrounded by an almost toroidally symmetric boundary. It has been found [28] that in this helical regime the helical ripple at the edge is relatively small, of the order of 1% of the total field, but still sufficient to spatially modulate local transport and kinetic properties [28–31].

In order to mimic a high current configuration and obtain a detailed edge investigation through the use of insertable probes, we discuss RFP discharges performed at lower plasma current ($I_p \leq 450$ kA) with a helical boundary ($m = 1$, $n = -7$) slowly and toroidally rotating at 10-15 Hz, which is externally applied via the feedback system. All the analyzed RFP discharges share the same equilibrium, with a common edge safety factor $q_a \approx -0.004$ and a normalized Greenwald fraction $n/n_G \leq 0.4$. Measurements are always referred to the flat top phase of the plasma current.

As already mentioned, RFX-mod is a highly versatile device: in addition to RFP operation, RFX-mod routinely operates as a circular low-field ohmic tokamak with the first wall representing the limiter [32]. The maximum plasma current achieved in tokamak operations is $I_p = 0.15$

MA, with a maximum toroidal magnetic field $B_\phi = 0.55$ T, corresponding to an edge safety factor $q_a = 1.7$. This low-q operations are possible only by means of a feedback control on the $(m = 2, n = -1)$ mode, that resonates close to the wall and would otherwise grow too large and disrupt the discharge [33]. In the following sections we present the results obtained by analyzing and reconstructing the topology in a typical tokamak discharge of RFX-mod, with $q_a \simeq 2.1$ and where a resonant (2, -1) perturbation with a rotation frequency of 10 Hz is applied through the feedback control system.

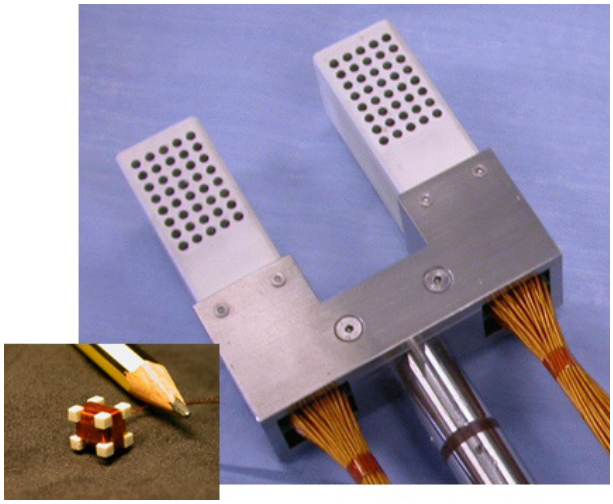

Figure 1: Picture showing the U-probe and a magnetic sensor.

In order to investigate the main features of transport and its effects on the plasma-wall interaction, insertable probes are extremely useful: in both configurations, the insertable *U-probe* [34], shown in Figure 1, has been exploited in low current discharges to avoid excessive heat load and damage to its components. The probe consists of two fingers, 88 mm apart along the perpendicular direction. In the tokamak configuration the probe is rotated by 90° according to the cross-field.

The U-probe provides detailed information about electrostatic and magnetic fluctuations in the boundary region of the plasma. In particular, it can be inserted radially up to 5 cm in the chamber, while it is located at fixed poloidal and toroidal position. In the RFP case, measurements are digitally sampled with a 0.2 μs time resolution while in the tokamak case the sampling frequency is half due to longer discharges. The U-probe exploits a modified triple-probe technique called *five-pin balanced triple probe* that has the advantage of reducing phase-shift problems between the signals [35]. This technique gives reliable measurements of floating potential ϕ_f, saturation current I_s and the electron temperature T_e. The floating potential is then related to the plasma potential ϕ_P by $\phi_P = \phi_f + \alpha T_e$. For the RFX deuterium edge plasma the constant α has

been estimated to be equal to 3.3 [36], in the approximation of ion temperature $T_i \simeq T_e$. The ion saturation current is related to the electron density n_e by $I_s = \beta n_e T_e^{1/2}$ where the constant β includes the effective probe collection area.

Thanks to the design of the probe, through a standard two-point technique [37] between subsequent perpendicularly spaced pins, it is possible to estimate the propagation of the fluctuations in the transversal direction. Thus, we can identify the transverse wave numbers that contribute to electrostatic-driven edge turbulence.

3. Topology studies

Theory and experiments are in agreement [28, 38] on the fact that the electrostatic properties of the plasma edge are modulated by the presence of magnetic islands: electrons are bounded to the magnetic field lines and they experience smaller drifts than ions, being less massive. This difference is more evident near island's fixed points (O- and X-points) and it is balanced by an ambipolar electric field which possesses the same symmetry of the parent island [39]. The ambipolar electric field produces an additional $\mathbf{E} \times \mathbf{B}$ flow, which can substantially modify edge transport.

In order to interpret edge data properly, a detailed discussion of the underlying topology is needed, for both the RFP and the tokamak configuration.

As mentioned in Section 2, we discuss the results of experiments where resonant MPs of definite helicity (m, n) are externally applied and slowly rotate in the laboratory frame of reference. Assuming that the magnetic island is rigidly rotating with the applied RMP, it is important to find a reference frame consistent with the rotation of the perturbation in order to infer the profiles of various transport-relevant quantities according to the underlying topology. To define the proper reference angle, the magnetic perturbations $\tilde{b}_r$ are Fourier analyzed and given by:

$$\tilde{b}_r(t) = \sum_{m,n} b_{m,n}(r) e^{i(m\theta + n\phi - \varphi_{m,n}(t))} \tag{1}$$

where $\varphi_{m,n}$ is the phase of the radial component of the perturbation measured by the experimental pick-up coils at the wall. From the sign convention adopted in the Fourier decomposition, the focus of our RFP analysis is on the ($m = 1$, $n = -7$) mode, which is the innermost resonant tearing mode for RFX-mod, while in the tokamak case we focus on the resonant ($m = 2$, $n = -1$) tearing mode.

Given the expression (1) for the Fourier decomposition of magnetic perturbations, the shift of

the last closed flux surface is $\sim \sin u$, with the *helical angle* defined by:

$$u_{m,n}(t) = m\theta + n\phi - \varphi_{m,n}(t) \tag{2}$$

This treatment for the RFP topology has already been discussed in [28] using the Hamiltonian formalism. As a consequence of the definition (2), for any applied perturbation and in any magnetic configuration, the O-point is always found at $u = \pi/2$, while the X-point is found at $u = 3\pi/2$. In panel *(b)* of Figure 4 the helical profile of the (1, -7) perturbation is visible for $r \leq 0.44$ m, together with the details of the toroidally coupled $m = 0$ island centered at $u = \pi$. In panel *(d)* of Figure 4 we show the magnetic topology reconstruction in the case of the tokamak configuration, where the helical profile of the (2, -1) perturbation is visible.

Therefore, using the helical angle defined in Equation (2), it is possible to translate the temporal information contained in $\varphi_{m,n}(t)$ to the fixed reference frame of the U-probe, when substituting ϕ and θ with the fixed angles at which the probe is located.

The topology reconstruction is then visualized through Poincaré maps of the edge, for example shown in the previously mentioned panels *(b)* and *(d)* of Figure 4. Poincaré plots are obtained through the field line tracing code FLiT [40]. Just outside the first wall of RFX-mod, a system of 48 (toroidal) and 4 (poloidal) sensors provides measurements of the fluctuations of the radial and toroidal components of the magnetic field. These measurements are used to reconstruct the eigenmodes in the plasma based on Newcomb's equation in toroidal geometry in a *force-free* assumption, following the model described in [41]. The NCT model applies to toroidal plasmas by solving a system of equations for the reconstruction of the mode eigenfunctions inside the whole plasma volume. These, in turn, are the inputs to the FLiT code that, following the eigenfunction integration, gives the trajectory of the magnetic field lines inside the plasma.

4. Electrostatic-driven transport and magnetic edge topology

Properties of transport driven by electrostatic fluctuations on the RFX-mod device are indeed modulated by the application of RMPs of definite helicity (m, n). In particular, the electric field radial profile and its dynamics have already been found to be highly influenced by the presence of edge magnetic islands [42]. It is worth reminding that a modulation in the presence of MP fields is also observed on the entire edge profiles: previous studies [21, 43] have indeed reported that the perpendicular flow is modulated along the helical angle, and this has been confirmed independently of the helicity of the dominant perturbation. Owing to the small contribution coming from the diamagnetic flow, the observed velocity modulation reflects the modification of the radial electric field, which has been theoretically explained in terms of ambipolar con-

straints [21].

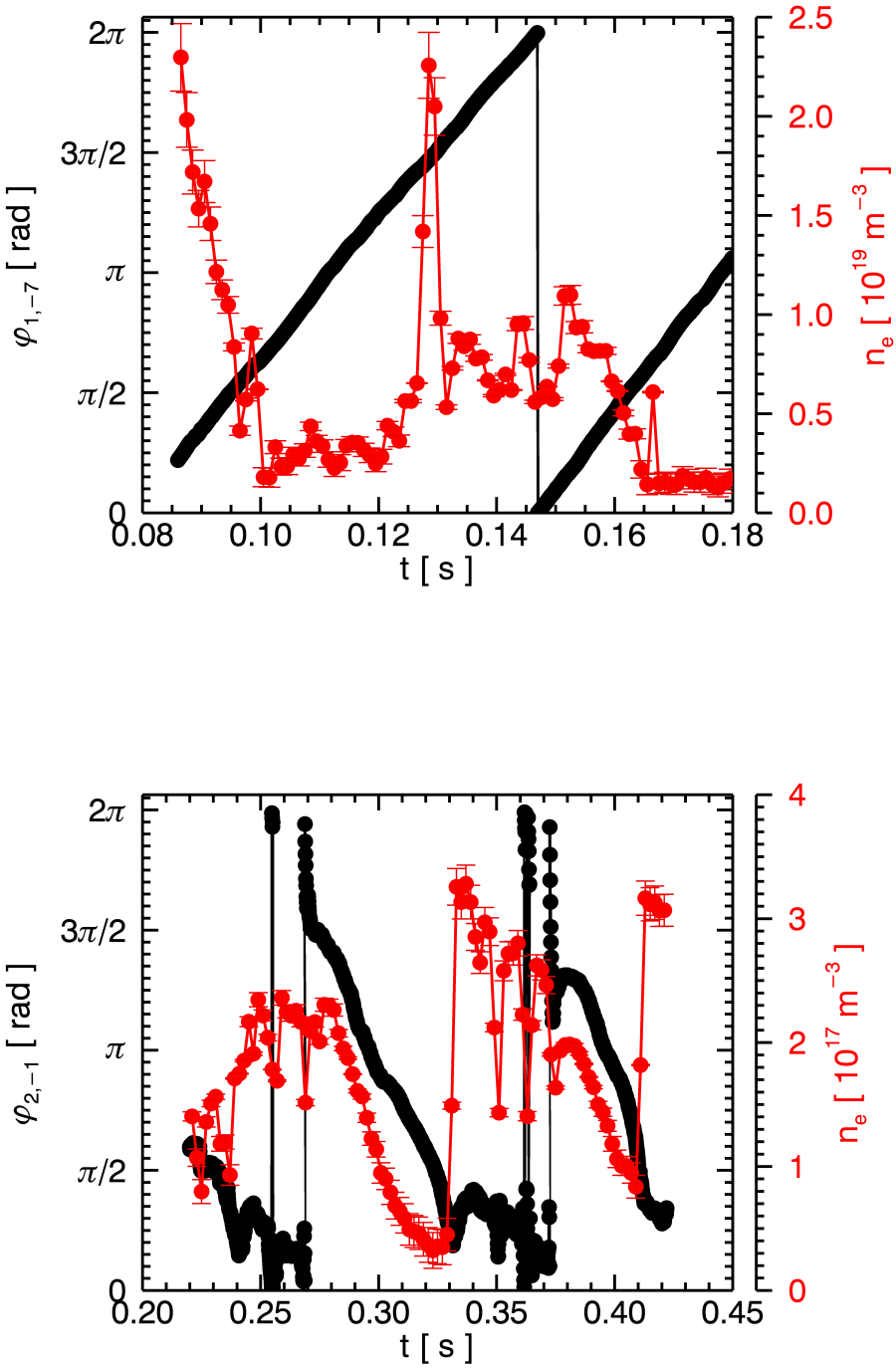

Figure 2: For RFP (top panel) and tokamak (bottom panel) experiments: the phase of the radial component of the externally applied magnetic field (black) and the electron density (red) are shown as a function of time.

In Figure 2 we show the phase of the radial component of the externally applied magnetic field $\varphi_{m,n}$ as a function of time, together with the edge electron density signal measured by the U-probe for both magnetic configurations implemented in RFX-mod.

In the $\varphi(t)$ profile we observe a complete rotation of the $(m = 1, n = -7)$ mode in the RFP case, while in the tokamak case two complete rotations of the $(m = 2, n = -1)$ mode are exhibited. It is worth noting that in the latter case the signal of the electron density shows a visible modulation following the $m = 2$ symmetry.

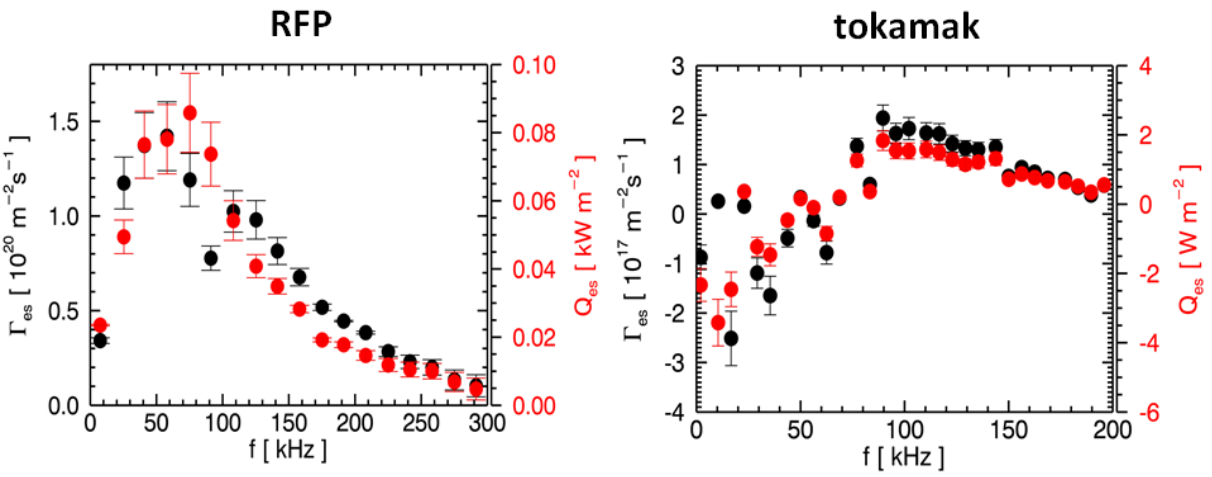

Figure 3: Electrostatic particle flux in black and energy flux in red in RFP case (left) and tokamak case (right) plotted as a function of the frequency. Each point represents the average of several measurements and the error bars represent the root mean square of measured values.

Particle fluxes have been obtained from the $\mathbf{E} \times \mathbf{B}$ component of the fluctuating radial velocity $\tilde{v}_r$ and electron density fluctuations $\tilde{n}_e$ [44]:

$$\Gamma_{es} = \langle \tilde{v}_r \tilde{n}_e \rangle = \frac{\langle \tilde{E}_\perp \, \tilde{n}_e \rangle}{B} \tag{3}$$

where $\tilde{E}_\perp$ represents the fluctuating electric field in the cross-field direction that in the RFP configuration coincides with the toroidal component, $\tilde{E}_\perp = \tilde{E}_\phi$, while in the tokamak case $\tilde{E}_\perp = \tilde{E}_\theta$. Furthermore, note that at the edge of a RFP the poloidal magnetic field B_θ is dominant whereas in the tokamak configuration $B \simeq B_\phi$. The electrostatic energy flux can be written as:

$$Q_{es} = \frac{3}{2} \langle \tilde{v}_r \tilde{p}_e \rangle = \frac{3}{2} \frac{\langle \tilde{E}_\perp \, \tilde{p}_e \rangle}{B} \tag{4}$$

where $\tilde{p}_e$ is the fluctuating electron pressure. Expressions (3) and (4) can be written in the Fourier space, i.e. the particle flux translates to [44]:

$$\Gamma_{es} = \frac{2}{B} \int_0^\infty k_\perp(\omega) \bar{n}(\omega) \bar{\phi}_p(\omega) \gamma_{n\phi}(\omega) \sin \alpha_{n\phi}(\omega) \, \mathrm{d}\omega \tag{5}$$

and an analogous expression can be written for Q_{es}.

In Equation (5), $\bar{n}$ and $\bar{\phi}_p$ are the square roots of the power spectra of density and plasma potential fluctuations, while $\gamma_{n\phi}$ is the coherence between them, $\alpha_{n\phi}$ is their relative phase and $k_\perp$ is the transverse wave number of the plasma potential fluctuations.

Most of the flux in RFP configuration is due to fluctuations with $f < 250$ kHz, in agreement with the results shown in [45] and as can be seen in the left panel of Figure 3. Spectral analyses in tokamak experiments have led us to evidence that particle and energy fluxes present an outward contribution mainly concentrated in the range 80 kHz $\leq f \leq$ 150 kHz and an *inward* contribution at $f < 80$ kHz, see right panel in Figure 3. This inward contribution in the electrostatic fluxes is not found in literature and will be subject of further investigations.

In the following, with respect to RFP analyses, we discuss data coming from an average performed over different discharges with similar plasma conditions and referred to the same radial insertion of $r/a \approx 0.97$, in the proximity of the maximum of the radial profile of Γ_{es}. On the other hand, data concerning tokamak analyses refer to a radial insertion of $r/a \approx 0.95$ and the results are relative to the modulation on the outward-directed contribution of the electrostatic fluxes.

A detailed magnetic reconstruction of the edge region is given in Figure 4 for both magnetic configurations on RFX-mod. As introduced in Section 3, we exploit Poincaré maps of the edge: in Poincaré plots of Figure 4, where panel *(b)* shows the RFP edge topology and *(d)* shows the tokamak one, every point is the intersection of a magnetic field line in the (r, $u_{1,-7}$) or the (r, $u_{2,-1}$) plane with a poloidal or toroidal chosen section. The color code in Poincaré plots indicates the initial condition in the radial coordinate of the magnetic field lines (blue = inner, red = outer). In panels *(a)* and *(c)* of Figure 4, we report the profiles of particle (black) and energy fluxes (red) as a function of the helical angle. It is worth recalling that in the RFP case the externally applied RMP (1, -7) modifies the edge plasma magnetic topology, giving rise, due to toroidal coupling with the Shafranov shift [41], to a chain of ($m = 0$, $n = -7$) magnetic islands resonating at the reversal surface. In the Poincaré plot in Figure 4 the profile of the (1, -7) perturbation is visible for $r \leq 0.44$ m, together with the details of the secondary $m = 0$ island centered at $u_{1,-7} = \pi$.

From the panels in Figure 4 it is possible to deduce that the average profiles of Γ_{es} and Q_{es} show the same periodicity of the applied RMP. In particular, the fluxes show a peak in the regions $\pi/2 \leq u_{1,-7} \leq 3\pi/2$ and $0 \leq u_{2,-1} \leq \pi$. If we compare this result to the Poincaré maps in Figure 4 *(b)* and *(d)*, the peaks are located in correspondence to the O-point of the outermost

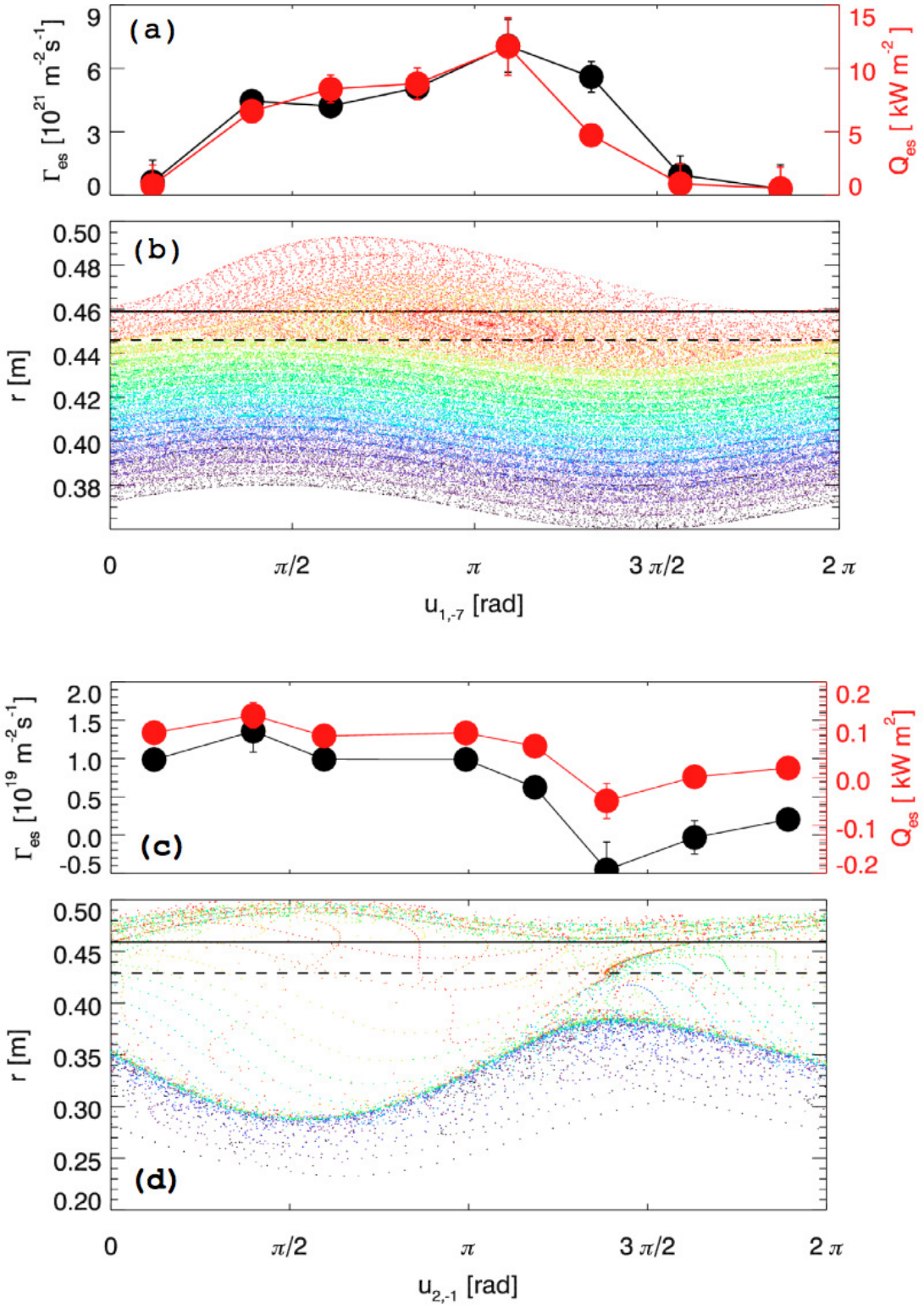

Figure 4: Poincaré plot in the plane (r, $u_{1,-7}$) for the RFP discharge # 35755 at $t = 0.139$ s *(b)*. Poincaré plot in the plane (r, $u_{2,-1}$) for the tokamak discharge # 35555 at $t = 0.3$ s *(d)*. The reconstructed topology is built in correspondence of a maximum of the externally applied perturbation. The black dashed line indicates the radial probe insertion while the black solid line defines the first wall. Above the Poincaré plots, the profiles of particle (black) and energy fluxes (red) are displayed as a function of the helical angle for the RFP *(a)* and tokamak *(c)* case.

resonating island: the (0, -7) island in the RFP case, the (2, -1) in the tokamak case.

5. Small scale electrostatic turbulence

The two-point technique allows the determination of the dispersion relation for the electrostatic fluctuations, which exhibit an almost linear relation in the region where most of the transport occurs. In both RFP and tokamak cases, fluctuations are found to propagate in the electron-diamagnetic direction.

On the basis of the experimental results and the reconstructed magnetic topology, it can be concluded that transport driven by electrostatic fluctuations is deeply affected by the RMP application. In particular, the induced magnetic perturbations lead to peaked profiles of transport relevant quantities in particular intervals of the helical angle: the electrostatic fluxes behave differently around the O-point and X-point of the outermost island which prompted us to investigate of the typical transverse wave numbers that contribute to these fluctuations.

Such analyses have been carried on a single typical discharge. The resulting profiles of Γ_{es} and Q_{es} can be observed in Figure 5: the blue dots represent the average profile around the O-point, while the red ones correspond to the profile around the X-point.

Looking at the profiles shown in Figure 5, the values of Γ_{es} and Q_{es} are definitely higher close to the O-point. Fluxes are shown as a function of the perpendicular wave number $k_\perp$ normalized to the ion gyroradius, $\rho_i = \frac{mv_\perp}{eB}$. In the RFP case we estimate $\rho_i \sim$ 2-3 mm while in the tokamak case $\rho_i \sim$ 1-2 mm.

In order to better understand the flux behavior in Figure 5, we have separately investigated the different contributions to the fluxes computation: in Figure 6 and in Figure 7 we show the power spectra of the electron density, the potential fluctuations and their relative phase $\alpha_{n\phi}$ (see Equation (5)) as a function of $k_\perp \rho_i$.

The RFP power spectra shown in Figure 6 suggest that bigger edge fluctuations, due $k_\perp \rho_i < 0.1$, are around the O-point region rather than in the X-point region. In the tokamak case, the reduction of density fluctuations is concentrated in the region, in terms of $k_\perp \rho_i$, where higher outward-directed flux is observed. In the lower region of the tokamak power spectra in Figure 6, due $k_\perp \rho_i < 0.02$, bigger fluctuations do exist around the X-point rather than the O-point but they do not effectively contribute to particle and energy transport, considering the range in $k_\perp \rho_i$ where the fluxes are peaked in Figure 5. From Figure 7, in the $k_\perp \rho_i$ range where the fluxes are peaked, we cannot infer any clear difference in the phase relation $\alpha_{n\phi}$ between the O-point and the X-point. On the other hand, the power spectra in Figure 6 confirm that the reason why the fluxes are lowered around the X-point region is clearly linked to a reduction in the fluctuation

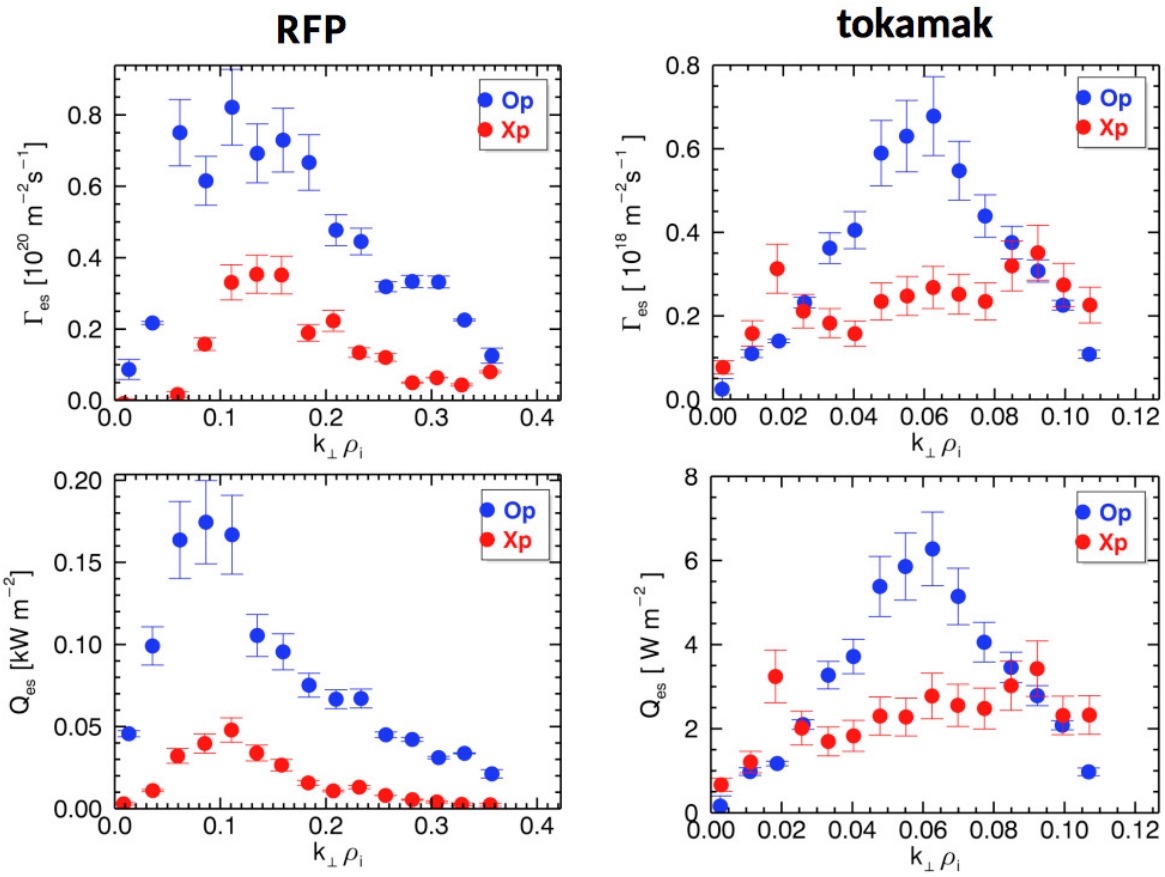

Figure 5: Profiles of electrostatic particle flux (top panels) and electrostatic energy flux (bottom panels) as a function of the transverse wave number $k_\perp$ normalized to the ion Larmor radius ρ_i. The blue dots represent data around the O-point of the perturbation, while the red ones correspond to the X-point.

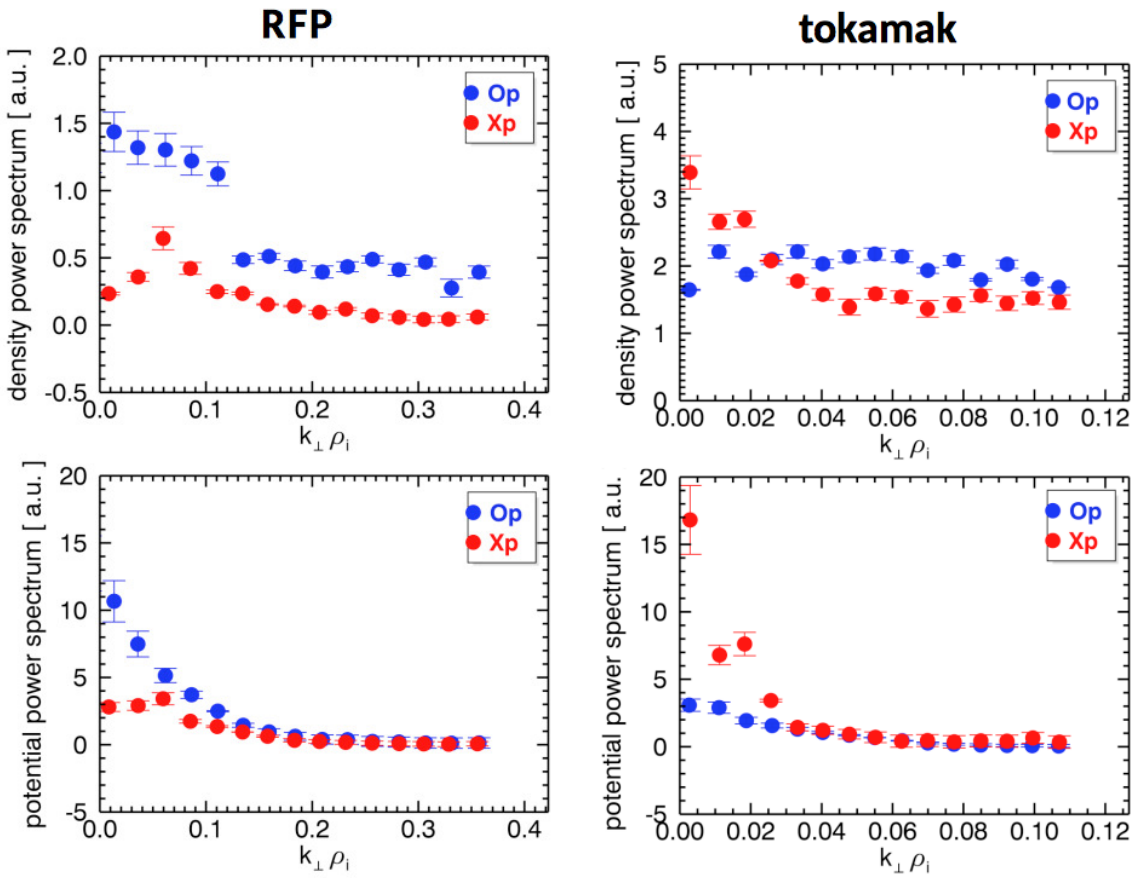

Figure 6: Power spectra of electron density $\bar{n}^2$ (top panels) and plasma potential $\bar{\phi}_P^2$ (bottom panels) fluctuations as a function of the normalized transverse wave number $k_\perp$. The blue dots represent data around the O-point of the perturbation, while the red ones correspond to the X-point.

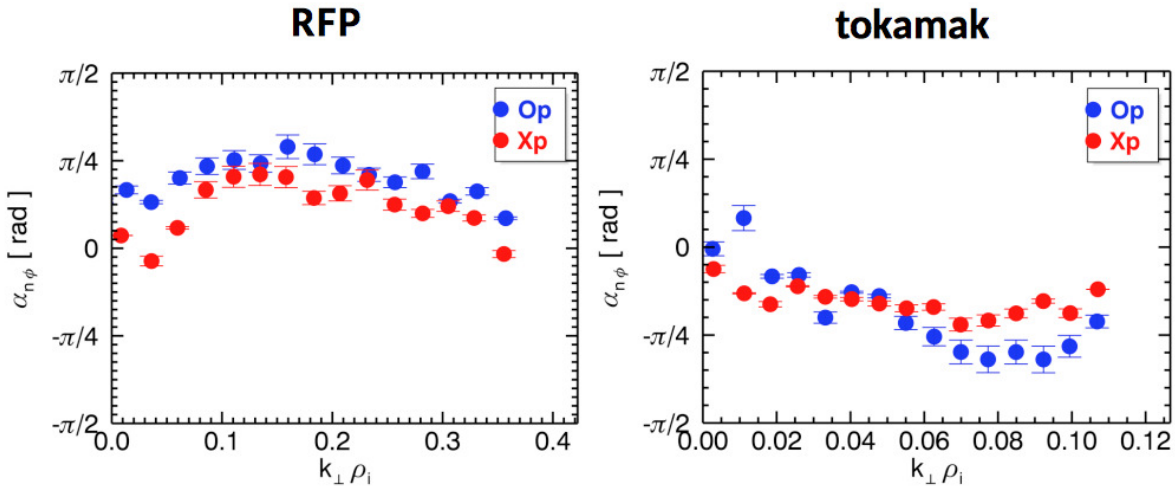

Figure 7: Relative phase between density and potential fluctuations. In the range where the the electrostatic fluxes shown in Figure 5 are peaked, $\alpha_{n\phi}$ profiles show no difference in the O-point and the X-point distributions.

amplitude in both RFP and tokamak case.

We have therefore given a specific description of transport around the O- and X-point regions of the applied perturbation: independently of the magnetic configuration and of the origin of fluctuations, transport is modulated with an increase close to the O-point. Transport scales are strongly reduced close to the X-point due to a reduction of fluctuations in a precise wave-vector space. We have indeed extracted the typical transverse wave numbers for the ρ_i-scale fluctuations of electrostatic particle and energy fluxes: $0.08 \leq k_\perp \rho_i \leq 0.2$ in the RFP case and $0.03 \leq k_\perp \rho_i \leq 0.09$ in the tokamak case.

6. Conclusions

In this paper we have discussed the modifications of transport channels at the edge of the RFX-mod plasma. These studies have been done both in RFP and in tokamak configuration, during experiments with application of external 3D magnetic perturbations.

The study of edge plasma transport properties requires measurements with high spatial and temporal resolution. The insertable U-probe has been exploited for this purpose, though its use is limited to low plasma current discharges to avoid damages to its components caused by an excessive heat load.

Analyses have been discussed in parallel in the RFP and the tokamak configuration, developing an analogy between the two magnetic configurations of the RFX-mod device.

Our investigations have included studies to relate transport properties with the underlying magnetic topology at the edge, exploiting Poincaré maps obtained through the field line tracing code FLiT. In the presence of rotating and resonant magnetic perturbations, measured plasma parameters exhibit a sinusoidal time evolution: this oscillatory behavior of the PWI as a function of time is better understood when the modulation on fluctuating values of transport properties is considered as a function of the local co-moving frame of reference. The choice of the helical angle as the meaningful reference frame is therefore consistent with the rotation of the perturbation, under the assumption of its rigid body rotation. Profiles of electrostatic particle and energy flux are found to follow the symmetry of the dominant imposed perturbation. Depletions in the profiles are found around X-point locations while enhancements correspond to the island's O-point, visible in the Poincaré maps.

It is important to underline that our major result is independent of the adopted magnetic configuration: the modulation of flux profiles manifests itself with an increase around the O-point of the outermost resonating island and a reduction in the X-point region due to the fluctuations level and not due to the relative phase. We can therefore deduce that the physics we have de-

scribed is common to both the reversed-field pinch and the tokamak configuration and involves multi-scale interactions and effects [46].

In terms of $k_\perp$, the spectra of the fluxes reveal that the transport contribution is due to fluctuations propagating in the electron diamagnetic drift direction peaked at $k_\perp \rho_i \sim 0.1$ in the RFP case and at $k_\perp \rho_i \sim 0.06$ in the tokamak case. The next step is to understand the quench of the fluctuations close to the X-point that eventually causes the reduction of the electrostatic fluxes. As future perspectives, we plan to have a simultaneous acquisition of current and potentials active on different rows of the U-probe, hence the possibility of extracting the electron density gradient. Through these probe's ameliorations, we will investigate possible driving mechanisms for the generation of poloidal turbulent flow as well as obtain information about the shear of the electric field in relation with the underlying topology.

In this paper, in both the RFP and the tokamak configuration, we have identified the transverse wave numbers contributing to ρ_i-scale turbulence at the edge. What is left to explore is the link with instabilities that drive turbulent transport: in other studies [47], drift and interchange instabilities have been found responsible of turbulent regimes at the plasma edge. A theoretical study would indeed be needed in order to fully understand the origins of electrostatic turbulence that drives transport at the edge in both reversed-field pinch and tokamak configuration.

Acknowledgment

This work has been carried out within the framework of the EUROfusion Consortium and has received funding from the Euratom research and training programme 2014-2018 under grant agreement No 633053. The views and opinions expressed herein do not necessarily reflect those of the European Commission.

References

[1] H Zohm. Edge localized modes (ELMs). *Plasma Physics and Controlled Fusion*, 38(2): 105, 1996. URL http://stacks.iop.org/0741-3335/38/i=2/a=001.

[2] J W Connor. Edge–localized modes – physics and theory. *Plasma Physics and Controlled Fusion*, 40(5):531, 1998. URL http://stacks.iop.org/0741-3335/40/i=5/a=002.

[3] W Suttrop. The physics of large and small edge localized modes. *Plasma Physics and Controlled Fusion*, 42(5A):A1, 2000. URL http://stacks.iop.org/0741-3335/42/i=5A/a=301.

[4] Y. Liang, H. R. Koslowski, P. R. Thomas, E. Nardon, B. Alper, P. Andrew, Y. Andrew,

G. Arnoux, Y. Baranov, M. Bécoulet, M. Beurskens, T. Biewer, M. Bigi, K. Crombe, E. De La Luna, P. de Vries, W. Fundamenski, S. Gerasimov, C. Giroud, M. P. Gryaznevich, N. Hawkes, S. Hotchin, D. Howell, S. Jachmich, V. Kiptily, L. Moreira, V. Parail, S. D. Pinches, E. Rachlew, and O. Zimmermann. Active control of Type–I Edge–Localized Modes with $n = 1$ perturbation fields in the JET Tokamak. *Phys. Rev. Lett.*, 98:265004, Jun 2007. doi: 10.1103/PhysRevLett.98.265004. URL http://link.aps.org/doi/10.1103/PhysRevLett.98.265004.

[5] Y Liang, H R Koslowski, P R Thomas, E Nardon, S Jachmich, B Alper, P Andrew, Y Andrew, G Arnoux, Y Baranov, M BÃl'coulet, M Beurskens, T Biewer, M Bigi, K Crombe, E De La Luna, P de Vries, T Eich, H G Esser, W Fundamenski, S Gerasimov, C Giroud, M P Gryaznevich, D Harting, N Hawkes, S Hotchin, D Howell, A Huber, M Jakubowski, V Kiptily, A Kreter, L Moreira, V Parail, S D Pinches, E Rachlew, O Schmitz, O Zimmermann, and JET-EFDA Contributors. Active control of type–I edge localized modes on JET. *Plasma Physics and Controlled Fusion*, 49(12B):B581, 2007. URL http://stacks.iop.org/0741-3335/49/i=12B/a=S54.

[6] W. Suttrop, T. Eich, J. C. Fuchs, S. Günter, A. Janzer, A. Herrmann, A. Kallenbach, P. T. Lang, T. Lunt, M. Maraschek, R. M. McDermott, A. Mlynek, T. Pütterich, M. Rott, T. Vierle, E. Wolfrum, Q. Yu, I. Zammuto, and H. Zohm. First observation of Edge Localized Modes mitigation with Resonant and nonresonant Magnetic Perturbations in ASDEX Upgrade. *Phys. Rev. Lett.*, 106:225004, Jun 2011. doi: 10.1103/PhysRevLett.106.225004. URL http://link.aps.org/doi/10.1103/PhysRevLett.106.225004.

[7] M.E. Fenstermacher, T.E. Evans, T.H. Osborne, M.J. Schaffer, J.S. deGrassie, P. Gohil, R.A. Moyer, and the DIII-D Team. Suppression of type–I ELMs using a single toroidal row of magnetic field perturbation coils in DIII–D. *Nuclear Fusion*, 48(12):122001, 2008. URL http://stacks.iop.org/0029-5515/48/i=12/a=122001.

[8] Keith H. Burrell Max E. Fenstermacher Ilon Joseph Anthony W. Leonard Thomas H. Osborne Gary D. Porter Michael J. Schaffer Philip B. Snyder Paul R. Thomas Jonathan G. Watkins William P. West Todd E. Evans, Richard A. Moyer. Edge stability and transport control with resonant magnetic perturbations in collisionless tokamak plasmas. *Nature Physics*, 2:419–423, 2006. doi: 10.1038/nphys312. URL http://www.nature.com/nphys/journal/v2/n6/full/nphys312.html.

[9] A. Kirk, I.T. Chapman, Yueqiang Liu, P. Cahyna, P. Denner, G. Fishpool, C.J. Ham, J.R.

Harrison, Yunfeng Liang, E. Nardon, S. Saarelma, R. Scannell, A.J. Thornton, and the MAST Team. Understanding edge-localized mode mitigation by resonant magnetic perturbations on MAST. *Nuclear Fusion*, 53(4):043007, 2013. URL http://stacks.iop.org/0029-5515/53/i=4/a=043007.

[10] Y. M. Jeon, J.-K. Park, S. W. Yoon, W. H. Ko, S. G. Lee, K. D. Lee, G. S. Yun, Y. U. Nam, W. C. Kim, Jong-Gu Kwak, K. S. Lee, H. K. Kim, and H. L. Yang. Suppression of Edge Localized Modes in High–Confinement KSTAR plasmas by nonaxisymmetric magnetic perturbations. *Phys. Rev. Lett.*, 109:035004, Jul 2012. doi: 10.1103/PhysRevLett.109.035004. URL http://link.aps.org/doi/10.1103/PhysRevLett.109.035004.

[11] J.M. Canik, R. Maingi, T.E. Evans, R.E. Bell, S.P. Gerhardt, H.W. Kugel, B.P. LeBlanc, J. Manickam, J.E. Menard, T.H. Osborne, J.-K. Park, S. Paul, P.B. Snyder, S.A. Sabbagh, E.A. Unterberg, and the NSTX team. ELM destabilization by externally applied non–axisymmetric magnetic perturbations in NSTX. *Nuclear Fusion*, 50(3):034012, 2010. URL http://stacks.iop.org/0029-5515/50/i=3/a=034012.

[12] P. B. Snyder, H. R. Wilson, J. R. Ferron, L. L. Lao, A. W. Leonard, T. H. Osborne, A. D. Turnbull, D. Mossessian, M. Murakami, and X. Q. Xu. Edge localized modes and the pedestal: A model based on coupled peeling–ballooning modes. *Physics of Plasmas (1994-present)*, 9(5):2037–2043, 2002. doi: http://dx.doi.org/10.1063/1.1449463. URL http://scitation.aip.org/content/aip/journal/pop/9/5/10.1063/1.1449463.

[13] M Lehnen, S Abdullaev, W Biel, M F M de Bock, S Brezinsek, C Busch, I Classen, K H Finken, M von Hellermann, S Jachmich, M Jakubowski, R Jaspers, H R Koslowski, A Krämer-Flecken, Y Kikuchi, Y Liang, A Nicolai, A Pospieszczyk, T Van Rompuy, U Samm, O Schmitz, G Sergienko, B Unterberg, R Wolf, O Zimmermann, and the TEXTOR team. Transport and divertor properties of the dynamic ergodic divertor. *Plasma Physics and Controlled Fusion*, 47(12B):B237, 2005. URL http://stacks.iop.org/0741-3335/47/i=12B/a=S18.

[14] E. Martines, R. Lorenzini, B. Momo, S. Munaretto, P. Innocente, and M. Spolaore. The plasma boundary in single helical axis RFP plasmas. *Nuclear Fusion*, 50(3):035014, 2010. URL http://stacks.iop.org/0029-5515/50/i=3/a=035014.

[15] Y Feng, M Kobayashi, T Lunt, and D Reiter. Comparison between stellarator and tokamak

divertor transport. *Plasma Physics and Controlled Fusion*, 53(2):024009, 2011. URL http://stacks.iop.org/0741-3335/53/i=2/a=024009.

[16] P.T. Lang, A. Loarte, G. Saibene, L.R. Baylor, M. Becoulet, M. Cavinato, S. Clement-Lorenzo, E. Daly, T.E. Evans, M.E. Fenstermacher, Y. Gribov, L.D. Horton, C. Lowry, Y. Martin, O. Neubauer, N. Oyama, M.J. Schaffer, D. Stork, W. Suttrop, P. Thomas, M. Tran, H.R. Wilson, A. Kavin, and O. Schmitz. ELM control strategies and tools: status and potential for ITER. *Nuclear Fusion*, 53(4):043004, 2013. URL http://stacks.iop.org/0029-5515/53/i=4/a=043004.

[17] S.C. McCool, A.J. Wootton, M. Kotschenreuther, A.Y. Audemir, R.V. Bravenec, J.S. DeGrassie, T.E. Evans, R.L. Hickok, B. Richards, W.L. Rowan, and P.M. Schoch. Particle transport studies with applied resonant fields on TEXT. *Nuclear Fusion*, 30(1):167, 1990. URL http://stacks.iop.org/0029-5515/30/i=1/a=014.

[18] S. Takamura, N. Ohnishi, H. Yamada, and T. Okuda. Electric and magnetic structure of an edge plasma in a tokamak with a helical magnetic limiter. *Physics of Fluids (1958-1988)*, 30(1):144–147, 1987. doi: http://dx.doi.org/10.1063/1.866180. URL http://scitation.aip.org/content/aip/journal/pof1/30/1/10.1063/1.866180.

[19] H. Stoschus, O. Schmitz, H. Frerichs, D. Reiser, M.W. Jakubowski, B. Unterberg, M. Lehnen, D. Reiter, U. Samm, and the TEXTOR team. Impact of rotating resonant magnetic perturbation fields on plasma edge electron density and temperature. *Nuclear Fusion*, 52(8):083002, 2012. URL http://stacks.iop.org/0029-5515/52/i=8/a=083002.

[20] N Vianello, C Rea, M Agostini, R Cavazzana, G Ciaccio, G De Masi, E Martines, A Mazzi, B Momo, G Spizzo, P Scarin, M Spolaore, P Zanca, M Zuin, L Carraro, P Innocente, L Marrelli, M E Puiatti, and D Terranova. Magnetic perturbations as a viable tool for edge turbulence modification. *Plasma Physics and Controlled Fusion*, 57(1):014027, 2015. URL http://stacks.iop.org/0741-3335/57/i=1/a=014027.

[21] G. Spizzo, N. Vianello, R. B. White, S. S. Abdullaev, M. Agostini, R. Cavazzana, G. Ciaccio, M. E. Puiatti, P. Scarin, O. Schmitz, M. Spolaore, D. Terranova, RFX, and TEXTOR Teams. Edge ambipolar potential in toroidal fusion plasmas. *Physics of Plasmas (1994-present)*, 21(5):056102, 2014. doi: http://dx.doi.org/10.1063/1.4872173. URL http://scitation.aip.org/content/aip/journal/pop/21/5/10.1063/1.4872173.

[22] M. Spolaore, M. Agostini, B. Momo, C. Rea, N. Vianello, M. Zuin, R. Cavazzana, G. De Masi, P. Innocente, L. Marrelli, E. Martines, A. Mazzi, M.E. Puiatti, S. Spagnolo, G. Spizzo, P. Scarin, D. Terranova, and P. Zanca. Turbulent electromagnetic filaments in actively modulated toroidal plasma edge. *Nuclear Fusion*, 2015. To be published.

[23] P. Sonato, G. Chitarin, P. Zaccaria, F. Gnesotto, S. Ortolani, A. Buffa, M. Bagatin, W.R. Baker, S. Dal Bello, P. Fiorentin, L. Grando, G. Marchiori, D. Marcuzzi, A. Masiello, S. Peruzzo, N. Pomaro, and G. Serianni. Machine modification for active MHD control in RFX. *Fusion Engineering and Design*, 66–68(0):161 – 168, 2003. ISSN 0920-3796. doi: http://dx.doi.org/10.1016/S0920-3796(03)00177-7. URL http://www.sciencedirect.com/science/article/pii/S0920379603001777. 22nd Symposium on Fusion Technology.

[24] L Marrelli, P Zanca, M Valisa, G Marchiori, A Alfier, F Bonomo, M Gobbin, P Piovesan, D Terranova, M Agostini, C Alessi, V Antoni, L Apolloni, F Auriemma, O Barana, P Bettini, T Bolzonella, D Bonfiglio, M Brombin, A Buffa, A Canton, S Cappello, L Carraro, R Cavazzana, M Cavinato, G Chitarin, S Dal Bello, A De Lorenzi, D F Escande, A Fassina, P Franz, G Gadani, E Gaio, E Gazza, L Giudicotti, F Gnesotto, L Grando, S C Guo, P Innocente, R Lorenzini, A Luchetta, G Malesani, G Manduchi, D Marcuzzi, P Martin, S Martini, E Martines, A Masiello, F Milani, M Moresco, A Murari, L Novello, S Ortolani, R Paccagnella, R Pasqualotto, S Peruzzo, R Piovan, A Pizzimenti, N Pomaro, I Predebon, M E Puiatti, G Rostagni, F Sattin, P Scarin, G Serianni, P Sonato, E Spada, A Soppelsa, G Spizzo, M Spolaore, C Taccon, C Taliercio, V Toigo, N Vianello, P Zaccaria, B Zaniol, L Zanotto, E Zilli, G Zollino, and M Zuin. Magnetic self organization, MHD active control and confinement in RFX–mod. *Plasma Physics and Controlled Fusion*, 49(12B): B359, 2007. URL http://stacks.iop.org/0741-3335/49/i=12B/a=S33.

[25] D. F. Escande, P. Martin, S. Ortolani, A. Buffa, P. Franz, L. Marrelli, E. Martines, G. Spizzo, S. Cappello, A. Murari, R. Pasqualotto, and P. Zanca. Quasi–Single–Helicity Reversed–Field–Pinch Plasmas. *Phys. Rev. Lett.*, 85:1662–1665, Aug 2000. doi: 10.1103/PhysRevLett.85.1662. URL http://link.aps.org/doi/10.1103/PhysRevLett.85.1662.

[26] S Cappello. Bifurcation in the MHD behaviour of a self-organizing system: the reversed field pinch (RFP). *Plasma Physics and Controlled Fusion*, 46(12B):B313, 2004. URL http://stacks.iop.org/0741-3335/46/i=12B/a=027.

[27] R. Lorenzini, E. Martines, P. Piovesan, D. Terranova, P. Zanca, M. Zuin, A. Alfier, D. Bonfiglio, F. Bonomo, A. Canton, S. Cappello, L. Carraro, R. Cavazzana, D. F. Escande, A. Fassina, P. Franz, M. Gobbin, P. Innocente, L. Marrelli, R. Pasqualotto, M. E. Puiatti, M. Spolaore, M. Valisa, N. Vianello, and P. Martin. Self-organized helical equilibria as a new paradigm for ohmically heated fusion plasmas. *Nat Phys*, 5(8):570–574, 08 2009. URL http://dx.doi.org/10.1038/nphys1308.

[28] N. Vianello, G. Spizzo, M. Agostini, P. Scarin, L. Carraro, R. Cavazzana, G. De Masi, E. Martines, B. Momo, C. Rea, S. Spagnolo, M. Spolaore, M. Zuin, and the RFX-Mod Team. 3D effects on the RFX–mod boundary. *Nuclear Fusion*, 53(7):073025, 2013. URL http://stacks.iop.org/0029-5515/53/i=7/a=073025.

[29] P. Scarin, N. Vianello, M. Agostini, G. Spizzo, M. Spolaore, M. Zuin, S. Cappello, L. Carraro, R. Cavazzana, G. De Masi, E. Martines, M. Moresco, S. Munaretto, M. E. Puiatti, M. Valisa, and the RFX-mod Team. Topology and transport in the edge region of RFX–mod helical regimes. *Nuclear Fusion*, 51(7):073002, 2011. URL http://stacks.iop.org/0029-5515/51/i=7/a=073002.

[30] M Agostini, P Scarin, G Spizzo, N Vianello, and L Carraro. Parallel and perpendicular structure of the edge turbulence in a three-dimensional magnetic field. *Plasma Physics and Controlled Fusion*, 56(9):095016, 2014. URL http://stacks.iop.org/0741-3335/56/i=9/a=095016.

[31] I.T. Chapman, D. Brunetti, P. Buratti, W.A. Cooper, J.P. Graves, J.R. Harrison, J. Holgate, S. Jardin, S.A. Sabbagh, K. Tritz, the MAST, NSTX Teams, and EFDA-JET Contributors. Three–dimensional distortions of the tokamak plasma boundary: boundary displacements in the presence of saturated MHD instabilities. *Nuclear Fusion*, 54(8):083007, 2014. URL http://stacks.iop.org/0029-5515/54/i=8/a=083007.

[32] P. Piovesan, D. Bonfiglio, F. Auriemma, F. Bonomo, L. Carraro, R. Cavazzana, G. De Masi, A. Fassina, P. Franz, M. Gobbin, L. Marrelli, P. Martin, E. Martines, B. Momo, L. Piron, M. Valisa, M. Veranda, N. Vianello, B. Zaniol, M. Agostini, M. Baruzzo, T. Bolzonella, A. Canton, S. Cappello, L. Chacón, G. Ciaccio, D. F. Escande, P. Innocente, R. Lorenzini, R. Paccagnella, M. E. Puiatti, P. Scarin, A. Soppelsa, G. Spizzo, M. Spolaore, D. Terranova, P. Zanca, L. Zanotto, and M. Zuin. RFX–mod: A multi–configuration fusion facility for three-dimensional physics studies. *Physics of Plasmas (1994-present)*, 20(5):056112, 2013. doi: http://dx.doi.org/10.1063/1.

4806765. URL http://scitation.aip.org/content/aip/journal/pop/20/5/10.1063/1.4806765.

[33] P. Zanca, R. Paccagnella, C. Finotti, A. Fassina, G. Manduchi, R. Cavazzana, P. Franz, C. Piron, and L. Piron. An active feedback recovery technique from disruption events induced by $m = 2$, $n = 1$ tearing modes in ohmically heated tokamak plasmas. *Nuclear Fusion*, 55(4):043020, 2015. URL http://stacks.iop.org/0029-5515/55/i=4/a=043020.

[34] M. Spolaore, N. Vianello, M. Agostini, R. Cavazzana, E. Martines, G. Serianni, P. Scarin, E. Spada, M. Zuin, and V. Antoni. Magnetic and electrostatic structures measured in the edge region of the RFX-mod experiment. *Journal of Nuclear Materials*, 390–391(0):448–451, 2009. ISSN 0022–3115. doi: http://dx.doi.org/10.1016/j.jnucmat.2009.01.132. URL http://www.sciencedirect.com/science/article/pii/S0022311509001548. Proceedings of the 18th International Conference on Plasma-Surface Interactions in Controlled Fusion Device Proceedings of the 18th International Conference on Plasma-Surface Interactions in Controlled Fusion Device.

[35] H. Y. W. Tsui, R. D. Bengtson, G. X. Li, H. Lin, M. Meier, Ch. P. Ritz, and A. J. Wootton. A new scheme for Langmuir probe measurement of transport and electron temperature fluctuations. *Review of Scientific Instruments*, 63(10):4608, 1992. doi: http://dx.doi.org/10.1063/1.1143683. URL http://scitation.aip.org/content/aip/journal/rsi/63/10/10.1063/1.1143683.

[36] V. Antoni, D. Desideri, E. Martines, G. Serianni, and L. Tramontin. Plasma flow in the outer region of the RFX reversed field pinch experiment. *Nuclear Fusion*, 36(11):1561, 1996. URL http://stacks.iop.org/0029-5515/36/i=11/a=I09.

[37] S.J. Levinson, J.M. Beall, E.J. Powers, and R.D. Bengtson. Space/time statistics of the turbulence in a tokamak edge plasma. *Nuclear Fusion*, 24(5):527, 1984. URL http://stacks.iop.org/0029-5515/24/i=5/a=001.

[38] M. Leconte, P.H. Diamond, and Y. Xu. Impact of resonant magnetic perturbations on zonal modes, drift-wave turbulence and the L–H transition threshold. *Nuclear Fusion*, 54 (1):013004, 2014. URL http://stacks.iop.org/0029-5515/54/i=1/a=013004.

[39] Gianluca Spizzo, Paolo Scarin, Matteo Agostini, Alberto Alfier, Fulvio Auriemma, Daniele Bonfiglio, Susanna Cappello, Alessandro Fassina, Paolo Franz, Lidia Piron,

Paolo Piovesan, Maria Ester Puiatti, Marco Valisa, and Nicola Vianello. Investigation on the relation between edge radial electric field asymmetries in RFX–mod and density limit. *Plasma Physics and Controlled Fusion*, 52(9):095011, 2010. URL http://stacks.iop.org/0741-3335/52/i=9/a=095011.

[40] P. Innocente, R. Lorenzini, D. Terranova, and P. Zanca. FLiT: A field line trace code for magnetic confinement devices. Submitted to Comput. Phys. Commun., 2015.

[41] Paolo Zanca and David Terranova. Reconstruction of the magnetic perturbation in a toroidal reversed field pinch. *Plasma Physics and Controlled Fusion*, 46(7):1115, 2004. URL http://stacks.iop.org/0741-3335/46/i=7/a=011.

[42] G. De Masi, E. Martines, M. Spolaore, N. Vianello, R. Cavazzana, P. Innocente, B. Momo, S. Spagnolo, and M. Zuin. Electrostatic properties and active magnetic topology modification in the RFX–mod edge plasma. *Nuclear Fusion*, 53(8):083026, 2013. URL http://stacks.iop.org/0029-5515/53/i=8/a=083026.

[43] G. Spizzo, M. Agostini, P. Scarin, N. Vianello, R. B. White, S. Cappello, M. E. Puiatti, M. Valisa, and the RFX-mod Team. Edge topology and flows in the reversed–field pinch. *Nuclear Fusion*, 52(5):054015, 2012. URL http://stacks.iop.org/0029-5515/52/i=5/a=054015.

[44] E.J. Powers. Spectral techniques for experimental investigation of plasma diffusion due to polychromatic fluctuations. *Nuclear Fusion*, 14(5):749, 1974. URL http://stacks.iop.org/0029-5515/14/i=5/a=020.

[45] E. Martines, V. Antoni, D. Desideri, G. Serianni, and L. Tramontin. Energy flux driven by electrostatic turbulence in the RFX edge plasma. *Nuclear Fusion*, 39(5):581, 1999. URL http://stacks.iop.org/0029-5515/39/i=5/a=302.

[46] Carlos Hidalgo. Multi-scale physics and transport barriers in fusion plasmas. *Plasma Physics and Controlled Fusion*, 53(7):074003, 2011. URL http://stacks.iop.org/0741-3335/53/i=7/a=074003.

[47] Bruce D. Scott. Drift wave versus interchange turbulence in tokamak geometry: Linear versus nonlinear mode structure. *Physics of Plasmas (1994-present)*, 12(6):062314, 2005. doi: http://dx.doi.org/10.1063/1.1917866. URL http://scitation.aip.org/content/aip/journal/pop/12/6/10.1063/1.1917866.